Theoretical study of cubic structures based on fullerene carbon clusters: $C_{28}C$ and $(C_{28})_2$

Linda M. Zeger, Yu-Min Juan, and Efthimios Kaxiras
Department of Physics and Division of Applied Sciences, Harvard University, Cambridge, Massachusetts 02138

A. Antonelli
Instituto de Fisica, Universidade Estadual de Campinas—Unicamp, Caixa Postal 6165, Campinas, São Paulo 13 081, Brazil
(Received 18 January 1995)

We study a hypothetical form of solid carbon $C_{28}C$, with a unit cell which is composed of the C_{28} fullerene cluster and an additional single carbon atom arranged in the zinc-blende structure. Using *ab initio* calculations, we show that this form of solid carbon has lower energy than hyperdiamond, the recently proposed form composed of C_{28} units in the diamond structure. To understand the bonding character of these cluster-based solids, we analyze the electronic structure of $C_{28}C$ and of hyperdiamond and compare them to the electronic states of crystalline cubic diamond.

I. INTRODUCTION

The C_{28} cluster has aroused considerable interest recently. This unit is the smallest fullerene that has been produced in significant quantities in experiments of laser vaporization of graphite.[1] The structure of C_{28} (Ref. 2) is shown in Fig. 1. The twelve pentagons and four hexagons that comprise this structure are arranged in a pattern that gives rise to three nearly tetrahedral bond angles around four apex atoms (two such atoms are marked by A in Fig. 1). Dangling sp^3 orbitals on the four apex atoms render this cluster chemically reactive. A C_{28} cluster forms a stable compound when it is produced with U, Ti, Zr, or Hf atoms trapped at its interior.[1,3,4]

There are three inequivalent sites on the C_{28} cluster: we refer to atoms at the apex sites as cage-A atoms, their immediate neighbors as cage-B atoms, and the ones that are not connected by covalent bonds to the cage-A atoms as cage-C atoms (see Fig. 1). It has been proposed that the C_{28} unit could be stabilized by externally saturating the dangling bonds of the four cage-A atoms with hydrogen.[1,5–7] Saturation of the dangling bonds through intercluster covalent bonding has also been considered: The four cage-A atoms of the C_{28} unit form the vertices of a tetrahedron, making the C_{28} unit analogous to a tetravalent atom. A natural choice for a crystal composed of these units is the diamond lattice.[1,8,9] This hypothetical solid called hyperdiamond and symbolized by $(C_{28})_2$, is shown in Fig. 2(a) in a perspective view. In Fig. 2(b), the same structure is shown with all the cage-A, cage-B, and cage-C atoms on a single (110) plane indicated.

A second candidate, which allows for tetrahedral bonding of C_{28} units, is a compound of C_{28} clusters and tetravalent atoms in the zinc-blende structure.[4] Since the hyperdiamond lattice contains large voids in its structure, one may expect that a solid composed of a more compact packing of C_{28} clusters alternating with individual tetravalent atoms, would be energetically more favorable. This kind of structure can be obtained by simply replacing the central cluster in Fig. 2 with a tetravalent atom and bringing the neighboring clusters closer to the central atom to form covalent bonds. In this paper, we consider a carbon atom as the second component of the zinc-blende structure. We have performed extensive first-principles calculations to give a detailed comparison between this zinc-blende structure and hyperdiamond. The results are also compared to cubic diamond.

The rest of this paper is organized as follows: Sec. II describes the computational approach used in our first-principles calculations. Section III demonstrates the energetic favorability of $C_{28}C$ over $(C_{28})_2$ through total energy comparisons. In Sec. IV, the electronic structure of $C_{28}C$ is discussed in detail and compared to that of diamond and of $(C_{28})_2$. Finally, in Sec. V, we draw con-

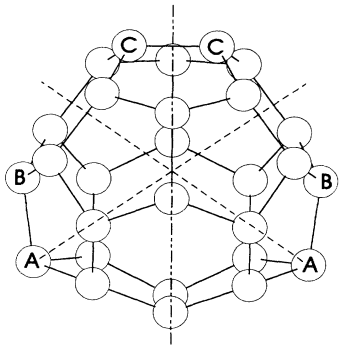

FIG. 1. Structure of the C_{28} unit. The dashed lines indicate two of the four axes of C_3 symmetry; the dashed-dotted line indicates one of the three axes of C_2 symmetry. The three atom types are (i) an apex or cage-A atom, where three fivefold rings meet; (ii) a cage-B atom, which is part of a sixfold ring and is bonded to a cage-A atom; and (iii) a cage-C atom, which is also part of a sixfold ring, but is not bonded to a cage-A atom.

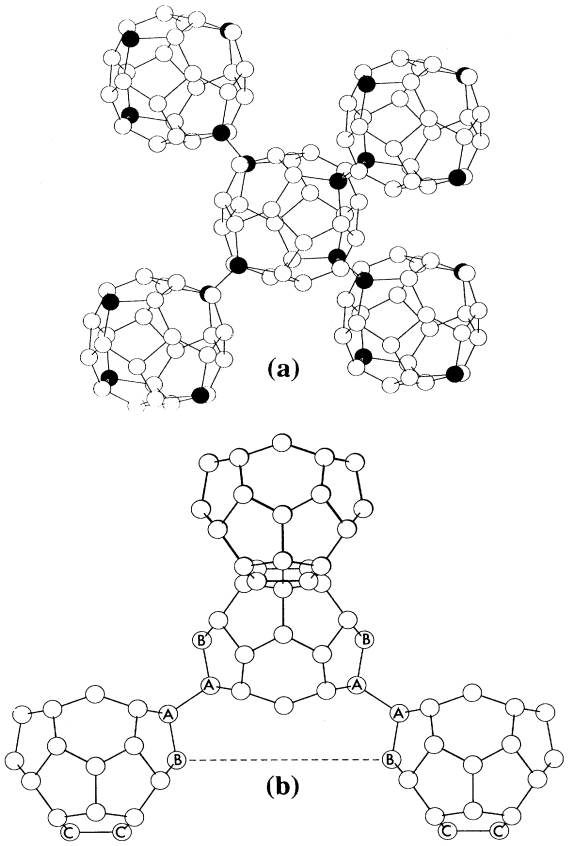

FIG. 2. (a) Perspective view of the structure of the hyperdiamond lattice. The C_{28} clusters are bonded together at the cage-A atoms shown here in black. (b) The same structure as (a) shown along a (110) crystallographic direction, where the positions of cage-A, cage-B, and cage-C atoms are indicated on a single plane. The dashed line indicates the place where weak intercluster B-B type bonding occurs in $(C_{28})_2$. The $C_{28}C$ structure is obtained by replacing the central cluster by a single C atom and bringing the neighboring clusters closer to that site to form covalent bonds. In that case, the interaction between neighboring cage-B atoms becomes much stronger (see text).

clusions on the new C_{28} based solids and comment on other possible solids based on similar cluster-atom combinations.

II. METHODS

We obtained total energies and electronic densities, as well as single particle electronic states and eigenvalues, by carrying out calculations within the framework of the density functional theory and the local density approximation (DFT/LDA).[10,11] The optimal atomic coordinates and the equilibrium lattice constants are obtained with a plane wave basis, including plane waves with kinetic energy up to 36 Ry. We also performed similar total energy calculations for bulk diamond, in order to make consistent total energy comparisons, and to obtain initial estimates for equilibrium bond lengths in $C_{28}C$. For the reciprocal space integration, the sampling k points have been chosen in a way such that the density of k points in the first Brillouin zone is kept approximately constant for all the structures we considered. For bulk diamond, we used 125 k points in the full Brillouin zone (which corresponds to eleven special points in the irreducible Brillouin zone),[12] with correspondingly smaller sets for the $C_{28}C$ and $(C_{28})_2$ structures. Within the molecular dynamics framework of Car and Parrinello,[13] we used the steepest descent method for the initial relaxation of the electronic degrees of freedom, followed by the more efficient conjugate gradient method close to the Born-Oppenheimer surface.

The ionic potential, including the screening from core electrons, was modeled by a nonlocal norm-conserving pseudopotential,[14] and the Kleinman-Bylander scheme[15] was employed to make the potential separable in Fourier space. The d angular momentum component was treated as the local part of the potential with the s and p components containing the nonlocal contributions.

The choice of lattice constant for the $C_{28}C$ lattice was guided by the diamond calculations. In $C_{28}C$, we first chose the length of the bond between the single carbon atom and the C_{28} cluster to be the equilibrium bond length of diamond, as obtained by our calculations. Since the interaction between cage-B atoms of neighboring C_{28} clusters can affect the optimal length of this C-C_{28} bond, we performed the calculations at several different lattice constants in the range near our initial choice, corresponding to different values for the C-C_{28} bond length, while the internal structure of the C_{28} cage was held fixed at the one determined by hydrogenation of the four cage-A atoms of the isolated cluster. We used this structure because the hydrogen atoms saturate the dangling bonds of C_{28} just as the single carbon atoms do in $C_{28}C$. By fitting to a Birch-Murnaghan equation of state,[16] we found that the lowest energy lattice constant corresponds to a C-C_{28} bond length of 1.53 Å. Fortuitously this was one of the actual lattice constants for which the $C_{28}C$ calculations were performed. For the optimal lattice so obtained, the positions of the atoms were then relaxed by minimizing the magnitude of forces obtained through the Hellmann-Feynman theorem. The cutoff below which the forces were considered to be negligible is 0.01 Ry/a.u. For the case of $C_{28}C$, this relaxation not only lowers the energy per atom but also changes the electronic structure from a metal to a semiconductor, which makes the crystal more stable. We discuss this further in Sec. IV. Similar calculation procedures were performed to obtain the optimal structure in $(C_{28})_2$.

III. THE RELATIVE TOTAL ENERGIES

The optimal total energy per atom for $C_{28}C$ and $(C_{28})_2$ after full relaxation is 0.453 eV and 0.744 eV, respectively, where we have used the energy per atom of diamond as the reference. The energy of $C_{28}C$ is lower than that of hyperdiamond, which is due in part to the presence of the additional fourfold coordinated carbon atoms (the added single carbon atoms). However, interclus-

ter interactions also play an important role in stabilizing $C_{28}C$. We can get an estimate of the effects of intercluster interaction by simply comparing the energy between a unit cell of $C_{28}C$ and the equivalent of twenty-eight atoms of $(C_{28})_2$ plus one atom of diamond: the $C_{28}C$ lattice is lower in energy by 0.26 eV per atom. This should be compared to the energy difference between $C_{28}C$ and $(C_{28})_2$ quoted above, which is 0.291 eV. Thus, intercluster interactions are more favorable in $C_{28}C$, rendering it lower in energy than it would be if the single added atoms were equivalent to diamond atoms and the C_{28} clusters were equivalent to those of $(C_{28})_2$.

We discuss next the effect of C_{28} cage relaxation on our results. The relaxation has decreased the energy per atom for the case of $C_{28}C$ by as much as 0.24 eV/atom, while only approximately 0.01 eV/atom is obtained through relaxation *from the same original choice of cage* (that of the hydrogenated C_{28} cluster) in the case of $(C_{28})_2$. In order to understand this, we first compare the distances between atoms in neighboring clusters between different structures and how relaxation affects them. In hyperdiamond, other than the covalent bond between cage-A atoms on neighboring clusters, the smallest distance between two atoms on neighboring clusters is between a cage-A atom on one cluster and a cage-B atom on the next cluster. This distance is 2.57 Å. The next smallest distance between atoms on neighboring clusters is between two cage-B atoms and has a value of 3.15 Å [see Fig. 2(b)]. In this case, relaxation does not induce any significant change on the geometry of the cage structure relative to the structure of the isolated, hydrogenated C_{28} cluster.

In contrast, in $C_{28}C$, the closest distance between atoms on neighboring clusters before relaxation is only 2.00 Å, between two cage-B atoms of the original cages. After the relaxation, this distance is reduced to 1.64 Å, which evidently introduces additional bonding between cage-B atoms, as we will see from the analysis of the electronic states in Sec. IV. Therefore, as far as the structural relaxation is concerned, we have observed significantly different behavior between $C_{28}C$ and $(C_{28})_2$. This was expected because the closest intercluster distance in the $C_{28}C$ solid occurs between two cage-B atoms, both of which are *threefold* coordinated. An additional B-B intercluster bond will be energetically favorable, as carbon atoms prefer to be fourfold coordinated in this environment. In the case of $(C_{28})_2$, the closest intercluster distance is between a cage-B and a *fourfold* coordinated cage-A atom, which makes the original cage structure in $(C_{28})_2$ electronically more stable compared to $C_{28}C$.

In Table I, we display the bond lengths of $C_{28}C$ and $(C_{28})_2$ before relaxation (the hydrogenated structure) and after relaxation. The relaxation in $(C_{28})_2$ produces lengthening of the intercluster bonds between cage-A atoms on neighboring C_{28} units and shrinking of all other intracluster bonds. The intracluster bonds, which are shortened by the largest amount, are those between cage-C atoms, which are the farthest bonds from the cage-A atoms. In the case of $C_{28}C$, a somewhat different relaxation pattern of the cage geometry emerged: the C-C_{28} bond and the C-C intracluster bonds were shortened, while the other two intracluster bonds were lengthened. This relaxation can be attributed to the formation of additional intercluster bonds between cage-B atoms.

IV. ELECTRONIC STATES

In Figs. 3(a), (b), and (c), we display the total valence electron densities of the fully relaxed $C_{28}C$ and $(C_{28})_2$ solids and diamond on the (110) plane. The length scales in Fig. 3 (a) and Fig. 3 (b) have been chosen so that these plots cover approximately equal areas. It is evident from a comparison of these figures that $C_{28}C$ has a higher atomic density than $(C_{28})_2$. Is is also apparent that the basic C_{28} cluster geometry remains essentially unchanged in both the $C_{28}C$ and $(C_{28})_2$ structures. This observation assures us that the C_{28} units are not altered significantly through the introduction of other C_{28} clusters or additional carbon atoms in the solid forms. The charge density around the additional carbon atom outside the cage [denoted by the symbol X in Fig. 3(a)] is seen to be similar to the intercluster A-A bond in $(C_{28})_2$. These bonds are single covalent bonds between two *fourfold* coordinated carbon atoms: comparison to Fig. 3(c) shows that they have the same bonding character as the bonds in bulk diamond. The main difference between $(C_{28})_2$ and $C_{28}C$ is the presence of additional bonds between cage-B atoms of neighboring clusters in the $C_{28}C$ crystal. These bonds, seen clearly in Fig. 3(a) between the two cage-B atoms of neighboring clusters, are somewhat weaker than regular covalent bonds, as expected from the fact that they are 1.64 Å long, compared to the 1.54 Å bond distance in bulk diamond.

TABLE I. Bond lengths before and after relaxation of the cage structure for both the $(C_{28})_2$ and $C_{28}C$ structures. The three types of intracluster bonds (bond A-B, B-C, and C-C) refer to the labels of atoms shown in Fig. 1 and Fig. 2(b).

Structure $(C_{28})_2$	Lattice constant (Å)	Bond A-B (Å)	Bond B-C (Å)	Bond C-C (Å)	C_{28}-C_{28} bond (Å)
Unrelaxed	15.777	1.525	1.412	1.507	1.504
Relaxed	15.777	1.510	1.407	1.479	1.539
Structure $C_{28}C$	Lattice constant (Å)	Bond A-B (Å)	Bond B-C (Å)	Bond C-C (Å)	C-C_{28} bond (Å)
Unrelaxed	9.685	1.525	1.412	1.507	1.530
Relaxed	9.685	1.574	1.469	1.435	1.501

In Fig. 4, we display the density of states (DOS) of $C_{28}C$ and $(C_{28})_2$ at the optimal lattice constants with full relaxation. The DOS of diamond, as calculated in this work, is also shown in dashed lines for comparison. The DOS of the cluster-based solids exhibit many features that can be related to features of the diamond DOS. For instance, the total valence bandwidth in all three cases is essentially the same, 21 eV. Some specific features deserve closer attention: In both cluster-based solids, the states corresponding to the intercluster bonding between cage-A atoms, which is similar in nature to the bonding in diamond, are far below the Fermi level. States immediately below and above the Fermi level derive from the bonding properties of atoms within the clusters. A careful examination of the symmetry of the wave functions of the highest occupied and lowest unoccupied states indicates that the states of $C_{28}C$ immediately below the Fermi level are due to a combination of intercluster bonding states between cage-B atoms and π bonding states between cage-C atoms within the clus-

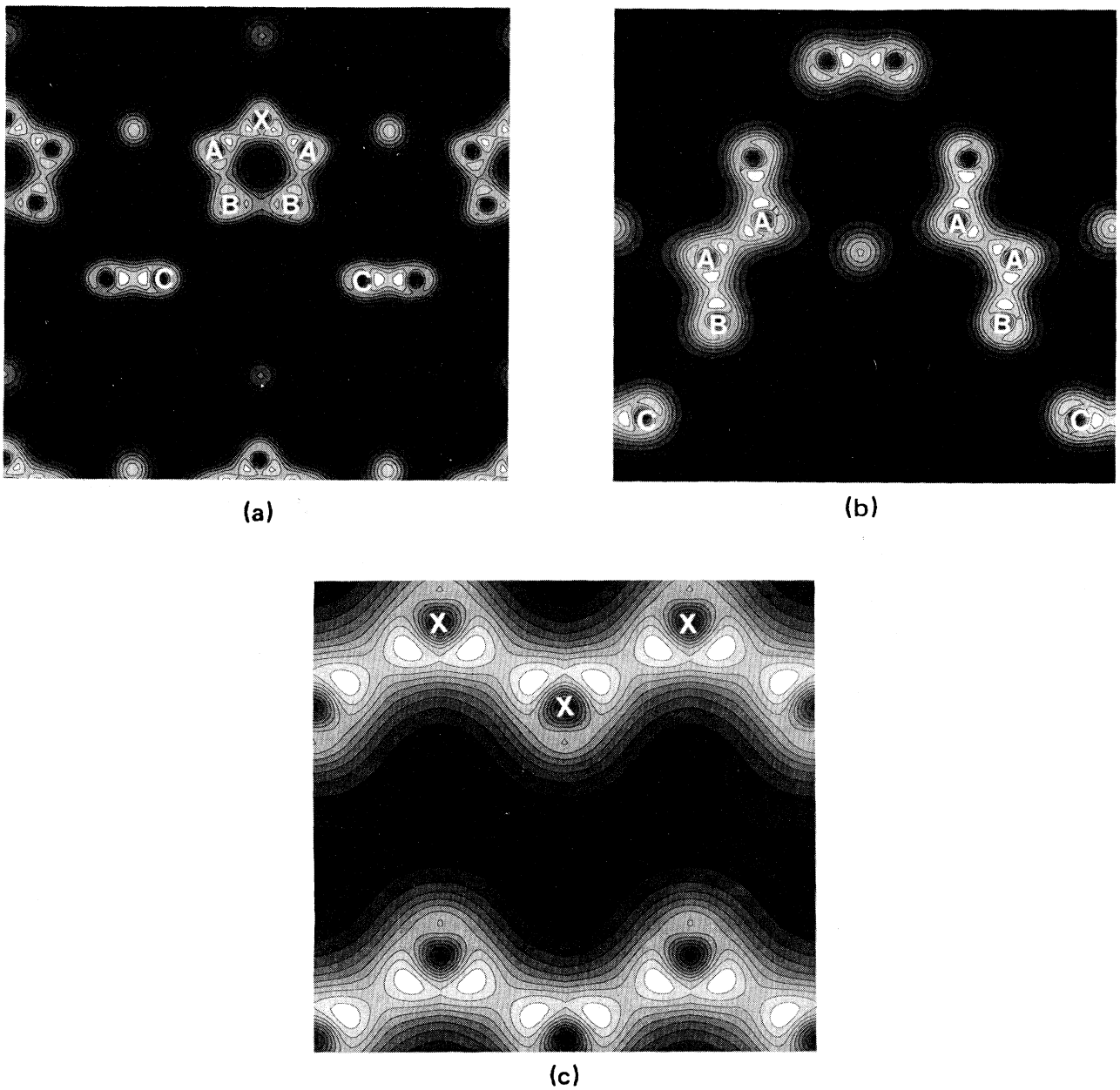

FIG. 3. Total valence electron density on the (110) plane of (a) $C_{28}C$, (b) $(C_{28})_2$, and (c) diamond. The white areas represent the highest electron density and the black areas the lowest. The positions of cage-A, cage-B, and cage-C atoms are shown in (a) and (b). The positions of the single extra carbon in $C_{28}C$ is indicated by the symbol X; the same symbol indicates the position of atoms in the diamond lattice (c).

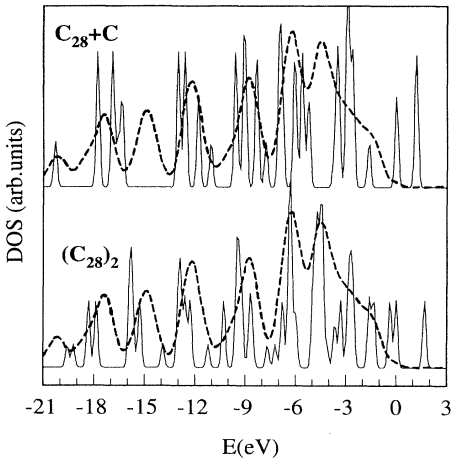

FIG. 4. Density of states vs energy for the $C_{28}C$ (upper part) and $(C_{28})_2$ (lower part) structures. For comparison, the density of states of diamond (as calculated here) is also shown in dashed lines. The Fermi level (top of the valence band) has been taken to be the zero of the energy scale for each structure.

ter. The same type of state involving intercluster bonding among cage-B atoms is responsible for the highest occupied state in $(C_{28})_2$, even though the interaction is much weaker in that case. On the other hand, the lowest unoccupied states in both solids are primarily due to a combination of intercluster bonding states between cage-B atoms and antibonding states between cage-C atoms within the cluster.

The DOS reveals that $(C_{28})_2$ is a semiconductor with direct band gap, which is consistent with results reported for $(C_{28})_2$ in previous works.[1,8,9] The fully relaxed $C_{28}C$ structure is also a semiconductor with direct band gap equal to 1.16 eV, approximately two thirds of the band gap of $(C_{28})_2$, and much smaller than the band gap of diamond. As we have noted above, there is a much stronger intercluster interaction in the case of $C_{28}C$ than in $(C_{28})_2$; it is, therefore, reasonable to expect that the electrons should be more delocalized in $C_{28}C$ than in $(C_{28})_2$, which leads to the smaller band gap of $C_{28}C$. Here, we wish to remind the reader of the well known inability of DFT/LDA to reproduce the experimental band gaps in semiconductors and insulators,[17] so that all the numbers quoted above are underestimates (by approximately a factor of 2) of the true band gaps, if these solids would be realized. For example, the band gap of crystalline cubic diamond obtained by the present calculation is 3.85 eV, which is approximately 2/3 of the experimentally measured value 5.52 eV.

V. CONCLUSIONS

In summary, we have studied two cluster-based solid structures, the $C_{28}C$ and $(C_{28})_2$ lattices. Both structures satisfy the condition that the dangling orbitals with sp^3 character on the cage-A atoms are fully saturated. Using first-principles calculations, we demonstrated that $C_{28}C$ is energetically preferred to $(C_{28})_2$. The crucial role of intercluster interactions at the cage-B atoms is revealed by the structural relaxation in $C_{28}C$, energetic comparisons, and the valence electronic charge density. The electronic structures of both $C_{28}C$ and $(C_{28})_2$ were analyzed. It was shown that for both solids, the intercluster bonding between cage-B atoms and π bonding between cage-C atoms within the cluster contribute to the highest occupied states in $C_{28}C$. The lowest unoccupied states, on the other hand, come from a combination of the cage-B type intercluster bonding states mentioned above and antibonding states between cage-C atoms within the cluster.

Just as intercluster interactions render $C_{28}C$ lower in energy than $(C_{28})_2$, other solids based on a C_{28} unit with saturated dangling bonds might be candidates for stable structures as well. For example, we expect that solids analogous to $C_{28}C$, but with the single C atom that links the C_{28} units replaced by other group-IV atoms (Si, Ge, Sn) would be equally stable, and with similar electronic properties. Alternatively, solid forms composed of C_{28} units connected by O atoms (chemical form $C_{28}O_2$) in a manner analogous to silica or crystalline forms of SiO_2 could be rather stable and somewhat easier to make, given the flexibility of packing of tetrahedra bonded at their corners. The conditions under which such solids may be experimentally realized remain to be investigated.

ACKNOWLEDGMENTS

The first-principles calculations were carried out at the Pittsburgh Supercomputer Center. This work was supported in part by the Office of Naval Research, Contract No. N00014-92-J-1138.

[1] T. Guo *et al.*, Science **257**, 1661 (1992).
[2] H. Kroto, Nature **329**, 529 (1987).
[3] B. I. Dunlap, O. Häberlen, and N. Rösch, J. Phys. Chem. **96**, 9095 (1992).
[4] M. Pederson and N. Laouini, Phys. Rev. B **48**, 2733 (1993).
[5] O.D. Häberlen, N. Rösch, and B. I. Dunlap, Chem. Phys. Lett. **200**, 418 (1992).
[6] T. Guo, R. E. Smalley, and G. E. Scuseria, J. Chem. Phys. **99**, 352 (1993).
[7] K. Jackson, E. Kaxiras, and M. Pederson, Phys. Rev. B **48**, 17566 (1993).
[8] D. Bylander and L. Kleinman, Phys. Rev. B **47**, 12345 (1993).
[9] E. Kaxiras, L. Zeger, A. Antonelli, and Y. Juan, Phys. Rev. B **49**, 8446 (1994).
[10] P. Hohenberg and W. Kohn, Phys. Rev. **136**, B864 (1964); W. Kohn and L. Sham, *ibid.* **140**, A1133 (1965).
[11] We use the expressions for the exchange-correlation functionals proposed by J. Perdew and A. Zunger, Phys. Rev. B **23**, 5048 (1984).
[12] H. J. Monkhorst and J. D. Pack, Phys. Rev. B **13**, 5188 (1976).

[13] R. Car and M. Parrinello, Phys. Rev. Lett. **55**, 2471 (1985).
[14] G. Bachelet, H. Greenside, G. Barraff, and M. Schlüter, Phys. Rev. **24**, 4745 (1981).
[15] L. Kleinman and D. M. Bylander, Phys. Rev. Lett. **48**, 1425 (1982).
[16] F. D. Murnaghan, Proc. Natl. Acad. Sci. U.S.A. **30**, 244 (1944); O. L. Anderson, J. Phys. Chem. Solids **27**, 547 (1966).
[17] J. Perdew and M. Levy, Phys. Rev. Lett. **51**, 1884 (1983); L. Sham and M. Schlüter, *ibid.* **51**, 1888 (1983); M. Hybertsen and S. Louie, *ibid.* **55**, 1418 (1985); R. Godby, M. Schlüter, and L. Sham, *ibid.* **56**, 2415 (1986).

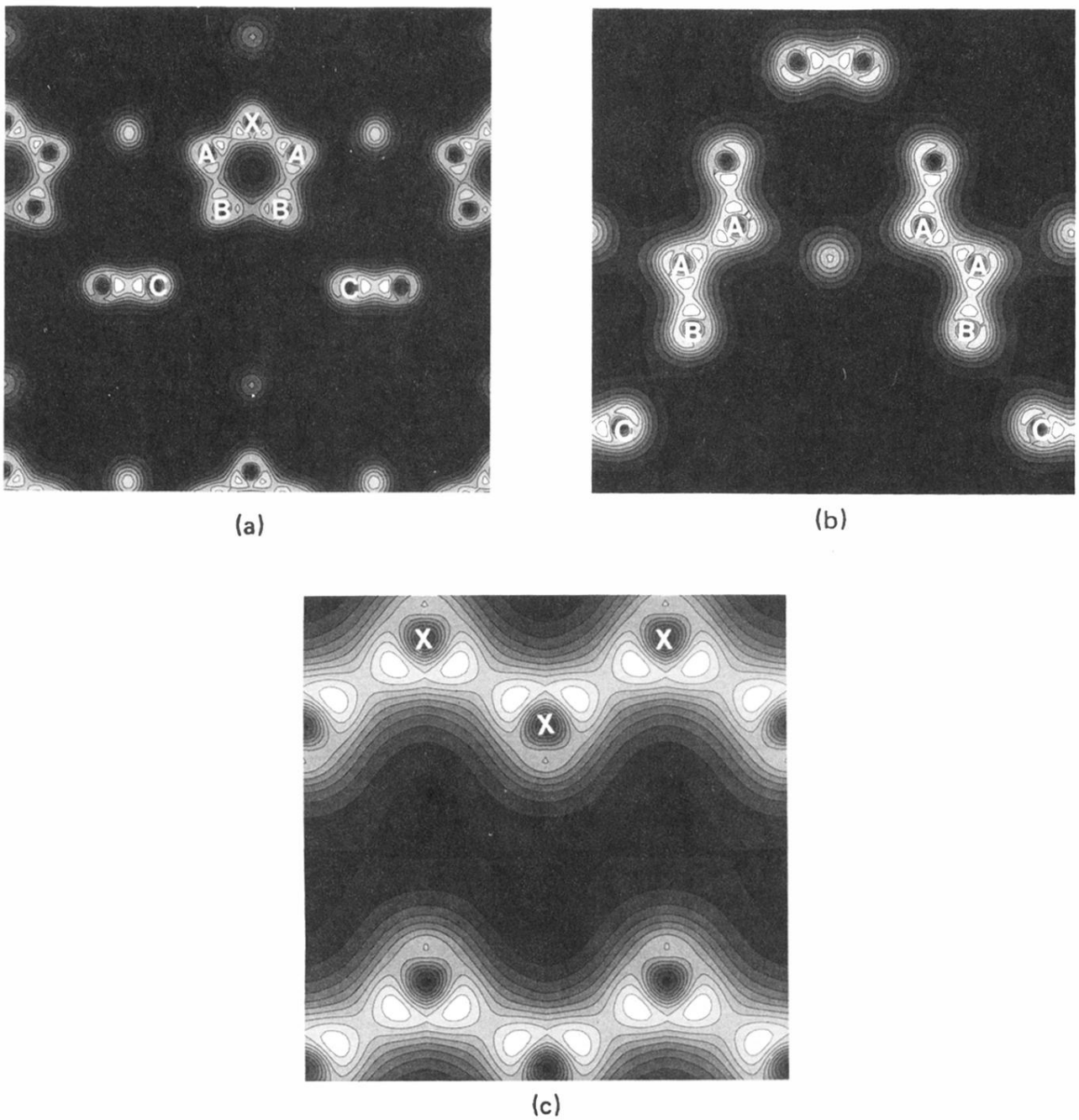

FIG. 3. Total valence electron density on the (110) plane of (a) $C_{28}C$, (b) $(C_{28})_2$, and (c) diamond. The white areas represent the highest electron density and the black areas the lowest. The positions of cage-A, cage-B, and cage-C atoms are shown in (a) and (b). The positions of the single extra carbon in $C_{28}C$ is indicated by the symbol X; the same symbol indicates the position of atoms in the diamond lattice (c).